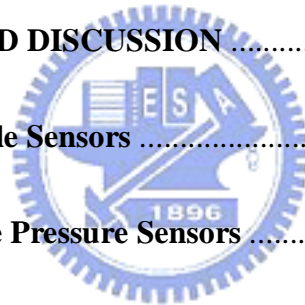


CONTENTS

ABSTRACT (CHINESE)	i
ABSTRACT (ENGLISH)	iv
ACKNOWLEDGMENTS	viii
CONTENTS	x
LIST OF TABLES	xiii
LIST OF FIGURES	xiv
NOMENCLATURE	xx
CHAPTER 1 INTRODUCTION	1
CHAPTER 2 PROPERTIES OF 6H-SiC	6
2.1 Crystal Structure of 6H-SiC	6
2.2 Elasticity and Piezoresistivity of 6H-SiC	8
CHAPTER 3 DESIGN AND SIMULATION OF THE SENSOR	17
3.1 Design of Piezoresistive Pressure Sensors Based on Circular Membrane with Center Boss Structure	17
3.1.1 Introduction	17
3.1.2 Analysis	19
3.1.3 Simulation and Discussion	30
3.2 Design of Piezoresistive Tactile Sensors Based on Circular Membrane	

with Center Boss Structure	40
3.1.1 Introduction	40
3.1.2 Analysis	42
3.1.3 Simulation and Discussion	49
CHAPTER 4 FABRICATION OF PRESSURE AND TACTILE SENSORS ..	55
4.1 Fabrication of PSOI Pressure and Tactile Sensors	55
4.2 Fabrication of 6H-SiC Pressure and Tactile Sensors	59
4.3 Package with High Temperature Adhesives	66
CHAPTER 5 RESULTS AND DISCUSSION	74
5.1 Piezoresistive Tactile Sensors	74
5.2 PSOI Piezoresistive Pressure Sensors	77
5.3 6H-SiC Piezoresistive Pressure Sensors	87
CHAPTER 6 CONCLUSIONS AND FUTURE WORKS	91
REFERENCES	96
APPENDIX A	106
A.1 Sample Preparation	107
A.2 Anodization Process	110
A.3 Oxidation Process	113
APPENDIX B	119



B.1 Sample Preparation	119
B.2 Constant Current Electrochemical Etching	121
B.3 Etching Profile	122



LIST OF TABLES

Table 2.1. 6H-SiC elastic stiffness	13
Table 2.2. 6H-SiC elastic compliance	13
Table 2.3. Published n-type 6H-SiC piezoresistive coefficients	15
Table 2.4. Published p-type 6H-SiC piezoresistive coefficients	16
Table 3.1. Properties of circular membranes with and without center boss structure	24
Table 4.1. Etching rate and roughness of 6H-SiC by RIE with different gas concentrations after 30 minutes	65
Table 4.2. Summary of the tested adhesives	70
Table 5.1. Characteristics of the PSOI piezoresistive pressure sensor	87
Table B.1 p-type 6H-SiC anodic etching rate (unit: $\mu\text{m}/\text{min}$) with respect to different HF concentration and current density	124

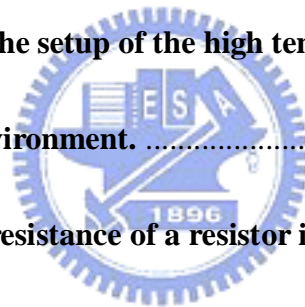
LIST OF FIGURES

Figure 2.1. Miller Index system for a hexagonal system.	6
Figure 2.2. Atom structure of 6H-SiC. Green (smaller) and blue (bigger) balls represent for carbon and silicon atoms, respectively.	8
Figure 2.3. Euler’s angles.	11
Figure 3.1. Three working conditions of a center boss pressure sensor: (a) the outer edge of the membrane is fixed and the center boss is free. (b) both the outer edge of the membrane and the center boss are fixed. (c) the outer edge of the membrane is fixed and the center boss has a distance from the bottom.	20
Figure 3.2. Arrangement of the piezoresistors on the center boss pressure sensor (a) top view of the sensor chip (b) the schematic view of the sensor.	25
Figure 3.3. Model used to analyze the deflection and stress distribution when both the outer edge of the membrane and the center boss are fixed.	28
Figure 3.4. Analytic solutions of Case (A) in comparison with FEM results for: (a) the distribution of the deflection and (b) longitudinal and transverse stress along the radial distance with respect to	

different ratios, n	32
Figure 3.5. Determination of the ratio of the radius of center boss to the	
radius of circular membrane by given Poisson's ratio.	34
Figure 3.6. Analytic solutions of Case (B) in comparison with FEM results for	
(a) the distribution of the deflection and (b) longitudinal and	
transverse stresses along the radial distance with respective to	
different ratios, n	36
Figure 3.7. Longitudinal stresses with respective to the ratio of the radius of	
the center boss to the radius of the circular membrane.	37
Figure 3.8. Sensitivity of Case (A) and Case (B) with respective to different	
ratios, n	38
Figure 3.9. Analytic solutions of Case (C) in comparison with FEM results for:	
(a) the distribution of the deflection, (b) longitudinal and (c)	
transverse stresses along the radial distance with respective to	
different pressures.	40
Figure 3.10. Cross section view of the proposed tactile sensor.	43
Figure 3.11. Deflection of the tactile sensor while an object contacts.	44
Figure 3.12. Model of the proposed tactile sensor (a) a circular membrane	
with center boss structure when the force, P, is applied to the	

center (b) an annular structure with the fixed inner and outer edge when the shear force, Q , is distributed along the inner edge uniformly.	48
Figure 3.13. Distribution of (a) the deflection and (b) longitudinal and (c) transverse stress with different n.	52
Figure 3.14. Longitudinal and transverse stresses at the inner and outer edge of the annular structure with respect to different ratios, n. ...	52
Figure 4.1. Fabrication process of the PSOI pressure and tactile sensor.	58
Figure 4.2. Photography of the fabricated pressure and tactile sensors. The background is a processed wafer with piezoresistors and metal lines. There are two chips, which show the circular membrane with center boss structure on the backside.	59
Figure 4.3. Process of 6H-SiC pressure and force sensors.	65
Figure 4.4. Photography of the fabricated 6H-SiC pressure and tactile sensors. The background is a 1 Euro cent.	66
Figure 4.5. Degradation of the pull-off force of the bonded wires during the 450°C treatment.	68
Figure 4.6. (a) Cross-section view and (b) top view of the package for the testing of the high temperature pressure sensor.	72

Figure 4.7. Photography of a packaged PSOI pressure sensor.	73
Figure 5.1. Setup of the characterization environment for the tactile sensor. ...	75
Figure 5.2. Measurement result of a PSOI piezoresistive tactile sensor at room temperature and supplying voltage 500mV.	76
Figure 5.3. Measurement results of a 6H-SiC tactile sensor at room temperature and supplying voltage 1V.	76
Figure 5.4. Setup of the high temperature pressure sensor measurement environment.	78
Figure 5.5. Photography of the setup of the high temperature pressure sensor measurement environment.	79
Figure 5.6. Variation of the resistance of a resistor in the PSOI pressure sensor's bridge with respect to temperature.	80
Figure 5.7. Characteristic of one PSOI pressure sensor with the adhesive, Epotek 526N, (a) the output voltage versus applied pressure with respect to different temperature (b) TCO and (c) TCS with respect to temperature.	84
Figure 5.8. Long-term stability test of PSOI pressure sensor at 10 bar and 250 °C.	85
Figure 5.9. Characteristic of the PSOI pressure sensor after the long-term	



test.	86
Figure 5.10. I-V curve of n-type 6H-SiC piezoresistors.	88
Figure 5.11. Temperature dependence of the resistance of an n-type 6H-SiC piezoresistor.	89
Figure 5.12. Output voltage of a 6H-SiC piezoresistive pressure sensor with respect to pressure and temperature.	89
Figure 5.13. TCO and TCS of a 6H-SiC piezoresistive pressure sensor.	90
Figure A.1. Main process steps of the etching process for n-type 6H-SiC.	107
Figure A.2. Preparation of n-type 6H-SiC samples to be etched.	109
Figure A.3. Setup for the n-type 6H-SiC electrochemical etching.	110
Figure A.4. Cross-section of an n-type 6H-SiC sample after 2 hour anodization (50mA/cm², 2%HF).	112
Figure A.5. Cross-section of an n-type 6H-SiC sample with a higer HF concentration.	113
Figure A.6. Cross-section of the anodized n-type 6H-SiC sample after 10 hours wet thermal oxidation.	115
Figure A.7. Appearance of the porous structure after 10 hours oxidation of 1150°C. The oxidized porous layer is then etched in an HF solution.	116

Figure A.8. Depth of the cavities V.S. anodization time. 116

Figure A.9. Photograph of an etched 6H-SiC cavity. 117

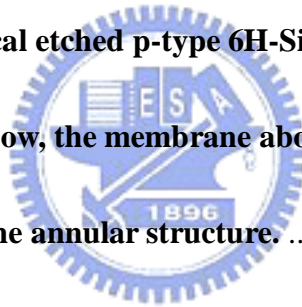
Figure A.10. Profile of the etched 6H-SiC cavity. 117

Figure A.11. Roughness of the n-type 6H-SiC surface after etching. 118

Figure B.1. Process flow for the preparation of p-type 6H-SiC samples. 121

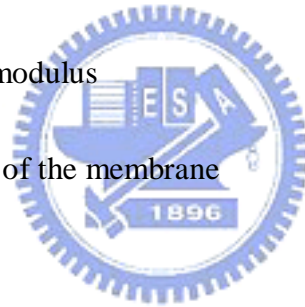
Figure B.2. Profiles measured by a profile meter (a) an anodic etched annular structure with a 200 μ m deep annular cavity (b) the roughness of the structure before anodic etching and (c) after anodic etching. ... 125

Figure B.3. An electrochemical etched p-type 6H-SiC annular structure. In the right-up window, the membrane about 20 μ m thick is magnified from the annular structure.126



NOMENCLATURE

a	: radius of the circular membrane
A	: area
b	: radius of the center boss
c_{ij}	: elastic stiffness coefficients
\mathbf{c}	: elastic stiffness tensor
D	: flexural rigidity
d	: distance for the over-range protection of a sensor
E	: Young's modulus
h	: thickness of the membrane
l	: length
n	: ratio between the radius of center boss and circular membrane
P	: contact force
q	: intensity load
q_{th}	: threshold pressure
Q	: shear force per unit length
r	: radial distance
R_1, R_2, R_3, R_4	: resistance of the four piezoresistors on a piezoresistive sensor



R_0	: resistance of the piezoresistor without stresses
$\Delta R_o, \Delta R_i$: change of the resistance at the outer and inner circumference of the annular membrane
s_{ij}	: elastic compliance coefficients
\mathbf{s}	: elastic compliance tensor
S	: sensitivity of the sensor
$w(x)$: distribution function of the deflection
σ	: stress tensor
$\sigma_r(x)$: distribution function of the longitudinal stress
$\sigma_t(x)$: distribution function of the transverse stress
σ_{ys}	: yield stress
ν, μ	: Poisson's ratio
η	: safe factor
ε	: strain
$\boldsymbol{\varepsilon}$: strain tensor
π_{ij}	: piezoresistance coefficients
$\boldsymbol{\pi}$: piezoresistance tensor
ρ	: resistivity

